International Journal of Nanoelectronics and Materials
Volume 16 January 2023 [21-32]

A Preliminary Study on Structural and Optical Properties of Heat Treated Nb_2O_5 Nanostructure

Evan. T. Salim[1,*], Jehan A. Saimon[1,**], Marwa K Abood [2], and Forat H. Alsultany[3]

[1]Applied Science Department, University of Technology-Iraq, Baghdad, Iraq
[2]Energy and Renewable Energies Technology Center, University of Technology-Iraq, Baghdad, Iraq.
[3]Al-Mustaqbal University College, Department of Medical Physics, Iraq

Received 18 January 2022, Revised 25 June 2022, Accepted 8 August 2022

ABSTRACT

Annealing is a heat treatment that alters the physical and sometimes chemical properties of a material to improve their crystalline structure and other important properties. This work presents the effect of post heat treatment on optical, structural, morphological, and surface roughness of Nb_2O_5 thin films at different temperatures (200-700°C) which to the best of our knowledge not been extensively studied yet. A clear modification in surface morphology and other studied properties was obtained. XRD results show a significant enhancement in the film's structural properties such as a reduction in the dislocation densities and stress. The optical properties of the treated films show a clear decrease in the transmission and energy gap values which their values were found to reduce from (4.35 to 2.9) eV with heat treatment up to 600°C and re-increase at 700°C. The surface roughness was also enhanced as a result of increasing the grain size from (9.95 – 34.7) nm Finally, SEM images of the films show an obvious change in their morphology and an increase in film uniformity as a result of heat treatment. Therefore, heat treatment could be considered as a helpful method to control film characteristics. Main result should be presented quantitatively.

Keywords: Nb_2O_5 thin film; precipitation method; heat treatment; XRD; optical properties; SEM.

1. INTRODUCTION

One of the best metal oxides with excessive potential is niobium oxide [1-3]. This material has emerged as a multi-application material and got a wide interest. It is one of the most important transparent oxides [4]. Several polymorphic crystalline shapes were recorded for this material depending on preparation conditions and methods [5]. The most popular structural phases are pseudo-hexagonal, orthorhombic, and monoclinic structures. In addition, the crystalline attitude of Nb_2O_5 material is affected by the raw materials used, synthesis processes, potential impurities, and any interaction with other components [6-8]. Many applications have been recorded for Nb_2O_5 as a functional material, such as sensors, catalysts, and elector-chromism [9-11].

The singular achievement of Nb_2O_5 in such studies produced the primary attention between investigators to scout additional capabilities of these metal oxides. In recent years, Nb_2O_5 has matured in publicity, and a diversity of morphologies extending from bulk crystals (large size) to various nanostructures have been advertised [12, 13]. Nanostructured Nb_2O_5 presents a rise to the surface to volume proportions and quantum confinement impacts in particular that permit unequaled chemical and physical interactions to take place at the surface [14-17].

* evan_tarq@yahoo.com, ** jehanedmon@gmail.com

More recently, attention to Nb_2O_5 has acquired extra activities because of implementations other than for catalysis and electro-chromism. For instance, thin films and nanostructures of Nb_2O_5 have been applied in solar cells, batteries, hetero detectors, and other electronic device applications [18-20].

Nb_2O_5 has been produced by employing several methods and the main motivation in selecting the correct production process is its ability to alter the Nb_2O_5 characteristics. These methods can be summarized as chemical vapour deposition, physical vapour deposition [21, 22], sol-gel, precipitation method, and thermal oxidation [23-26]. The sol-gel method involved a chemical reaction between a precursor containing (Nb+5) and ammonia aqueous solutions [27]. Nb_2O_5 represents a fairly unreactive and insoluble solid and only melts infused - alkali and it is dissolved with the hydrofluoric acid [28, 29].

The following chemical reaction represents the first process between the niobium oxides and hydrofluoric acid:

$$Nb_2O_5 + 10HF \rightarrow 2H_2\left[NbOF_5\right] + 3H_2O \quad (1)$$

Additional ammonia was added to the niobium fluorides solution, and Nb_2O_5 was precipitated according to the equation [28, 30]:

$$2H_2[NbOF_5] + 10NH_4OH \rightarrow Nb_2O_5 \downarrow + 10NH4F + 7H_2O \quad (2)$$

The product of this chemical reaction is pure Nb_2O_5 nano powders.

In this work, high quality Nb_2O_5 thin film was achieved at a specific annealing temperature, where the effects of different temperatures on the physical properties of niobium oxide films were investigated.

2. MATERIAL AND METHODS

Ultra-high purity niobium pentoxide 99.99% with (0.2 g) powder was dissolved in the HF under 100 ˚C water bath. The obtained solution was continuously stirred for about 1 hour until the solution was transparent. The process of chemical reaction was presented in equation (1). Ethanol and Double Ionized Water (DIW) were then added to dilute the solution. The next steps included adding 12 mol/L molarity of ammonium hydroxide, and as a result; niobium pentoxide colloidal solution was obtained as shown in equation (2). Spin coating technique was employed for film growth using (HOLMARC HO-TH-05) system at 2000 rpm, and 1.5 min duration. The prepared film layers were dried at 150˚C, for 15 min. This process was performed three times. The thickness of the film was measured using an optical scanning reflectometer from (Filmetrics F20, USA). Heat treatment includes different temperatures where the heating rate was increased to 10°C per min , the treated ranges are from 200 ^{o}C -700 ^{o}C.

The structural properties were investigated by using X-ray diffraction techniques that is Shimadzu 6000 X-ray diffract meter model. The structural constants were estimated by using equations (3-5) [31-34]:

$$D = \frac{0.9\lambda}{\beta \cos\theta} \quad (3)$$

$$\delta = \frac{1}{D^2} \tag{4}$$

$$\varepsilon = \frac{\beta}{4\tan\theta} \tag{5}$$

Where D is grain size (nm), θ is Braggs angle (deg), β is full width at half maximum (rad) δ is the density of dislocation and, ε is microstrain [35-38].

The thin film was deposited on a silicon substrate and the surface morphology was investigated by scanning electron microscopy (SEM). The material composition was determined by using (EDS / SEM) Tescan VEGA3 (AA-3000 model, Angstrom Advanced Inc, USA).

In order to measure the optical transmission, Nb2O5 thin films were deposited on quartz substrates. A UV-Vis spectrophotometer from a T60 model was used for this purpose. The optical parameters such as energy gap (Eg) were found using the following equation [39-41]:

$$(\alpha h\nu) = B(h\nu - Eg)^{1/2} \tag{6}$$

hν = incident photon energy, B = constant, absorption coefficient = a [42-44].

$$\alpha = \frac{1}{t}\ln\frac{1}{T_{rans}} \tag{7}$$

3. RESULTS AND DISCUSSION

3.1 Morphological Study

The morphological properties results of the films were obtained by using SEM as shown in Figure (1 a-f). It shows a clear re-crystallization of the surface morphology as a function of temperature. A transformation in the surface morphology was observed where a change from separated isolated islands Figure 1 (a) to network-like structures Figure 1 (b) with the heat treatment up to 200°C. Additional increase in temperature to 400°C the entanglement in the texture increased as shown in Figure 1 (c). A relative additional increase in temperatures up to 500 °C shows compact neighbouring particles with no space between them with a wide particle size range as presented in Figure 1 (d). When the temperature reached 600°C, a homogenous and fine structure could be recognized with relatively greater grain size as shown in Figure 1 (e). Rising the temperatures to 700°C led the film morphology to be completely changed to non -uniform rough surface as shown in Figure 1 (f).

The increase of pores and surface roughness may be related to the movement of the atoms or molecules on the film surface as the films annealed to a higher temperature. Due to annealing, some smaller grains or crystals diffuse and coalesce together to effectively form larger crystalline grains with clear crystallographic faces. The mentioned results above demonstrate that the process of annealing induces two parallel grain growth processes – one within the volume of the thin film matrix – a primary growth process, and the other over the thin film surface – a secondary growth process that resulted in various surface morphologies, surface porosity and structural properties as shown previously. When annealing temperatures were low, grain growth was relatively weak. With the increase of annealing temperatures, atoms diffusion was promoted, and more deformation energy storage was released, and the driving force of recrystallization

increased, thus improving the nucleation rate and hence the porosity increased due to the atom agglomerations [45, 46]

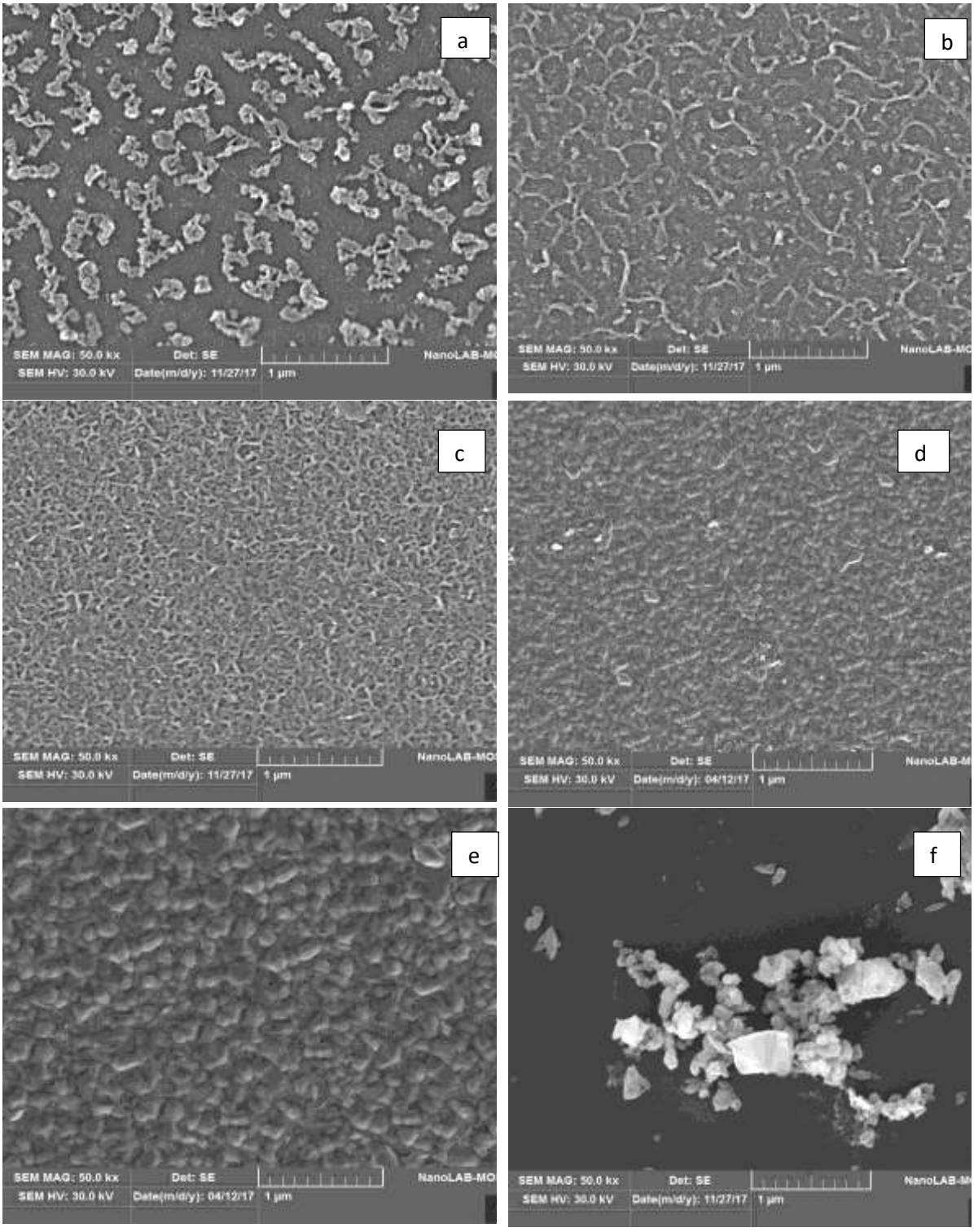

Figure 1. (A-G)SEM results of Nb_2O_5 thin films treated at (RT_700°C) respectively.

Figure 2 presents the EDS results of thin films treated at various temperatures. The obtained spectra ensure the presence of Nb and O elements with the strong silicon peak that was related to the substrate. At zero keV an intensive peak appeared on the x- axis is attributed to the device noise [47].

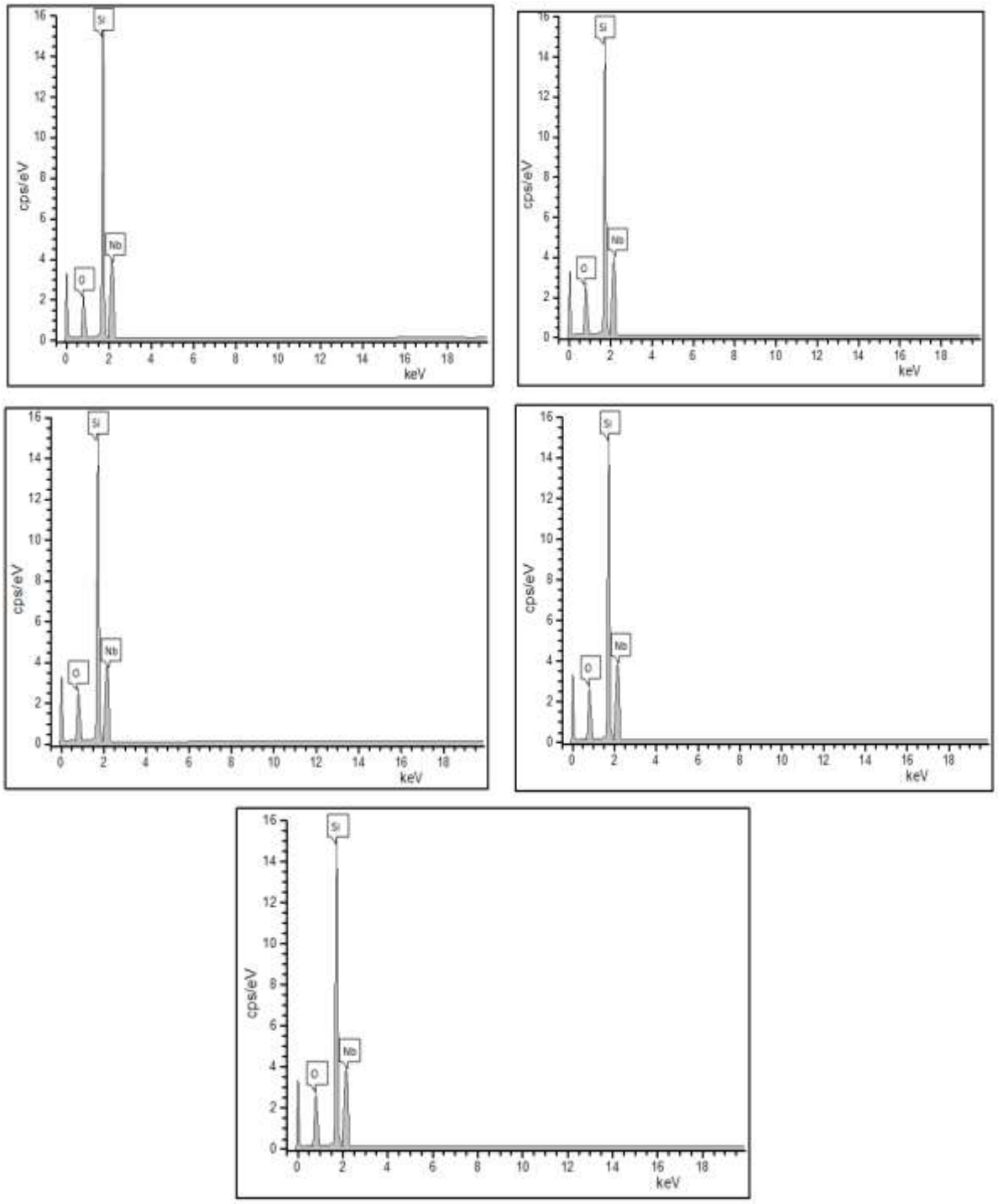

Figure 2. EDS results of Nb_2O_5 films after heat treatment at a range of temperatures (a-e) (200°C-700°C) respectively.

The Nb/O ratio as a function of treatment temperature is tabulated in Table 1, the reduction in the ratio from 1.77 to 1.7 with temperature was attributed to the increase in the adsorbed oxygen in the films as a result of the treatment. As a result, a decrease in the material stoichiometry from 76.2% to 72.98% as the temperatures increased from 200°C to 700°C.

Table 1 Stoichiometry, mass percentage of Nb and O extracted from EDS result analysis

Treatment temperature (°C)	Nb Wt%	O Wt%	Nb/O	Stoichiometry
200	63.97	36.03	1.77	76.20
400	63.5	36.5	1.73	74.66
500	63.4	36.6	1.74	74.34
600	62.98	37.02	1.701	73.01
700	62.97	37.03	1.700	72.98

3.2 Optical Properties

The optical properties of the films were investigated and the results is shown in Figure 3. The reduction in the transmission with the temperature is clear up to 600 °C, which is related to the oxygen vacancies presence. The oxygen defects increase the localized state's concentration in the band structure as similarly found in other work [48]. It was also attributed to the scattering from the grain boundary as the grain size increased with temperatures as shown in XRD results. The grain size increase also resulted in transmission decrease by increasing the absorption due to the reduction in the mechanical stress, because of the lattice distortion in the grain boundary regions which influence the electronic structure, hence, the below-band-edge optical absorption [49]. When the treatment temperatures increased beyond 600°C the transmission increased. In general, the increase of annealing temperature will increase the pores in films, which results in the decrease of refractive indices and increase of extinction coefficients of the film hence affecting the optical absorption and transmission of the films.

By using eq. (6), the energy gap was extracted at different temperatures as shown in Figure 4. An optical energy gap value could be recognized with temperatures. The band gap starts to decrease slightly when the temperature increases hence the re-crystallization begins. The reduction can be related to the unsaturated bonds which are responsible for the localized tail states formation in the energy gap as presented in Figure 5. The increase in these states is responsible for the band gap reduction. Additional raise in the annealing temperature to 700 °C resulted in the separation of the crystallites into smaller crystallites. In this case, the dangling bonds on the surface that is responsible for defects creation, which led to a reduction in the energy gap [50].

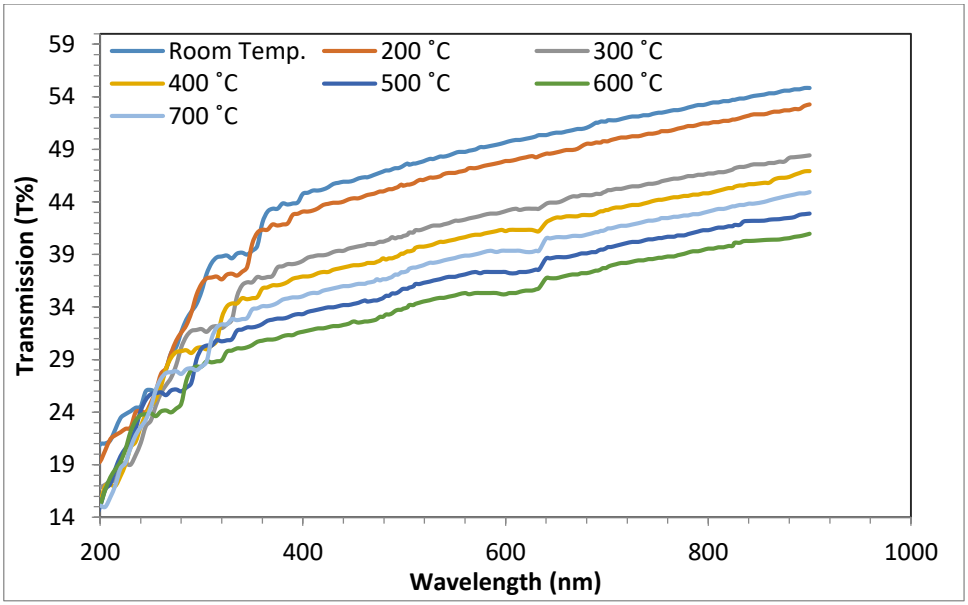

Figure 3. Optical transmission of Nb_2O_5 thin films at different treatment temperatures.

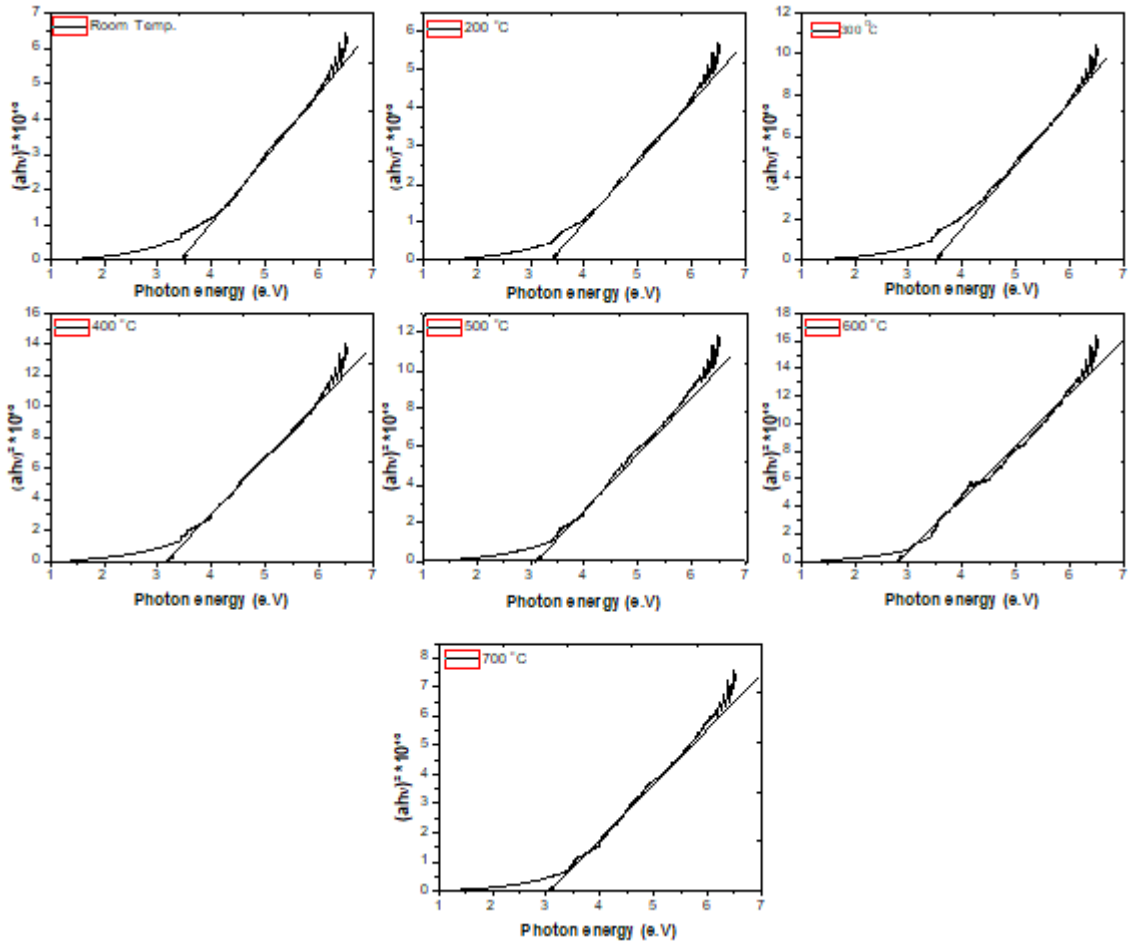

Figure 4. (A-G) Energy gap of Nb_2O_5 thin films prepared at (RT-700°C) respectively.

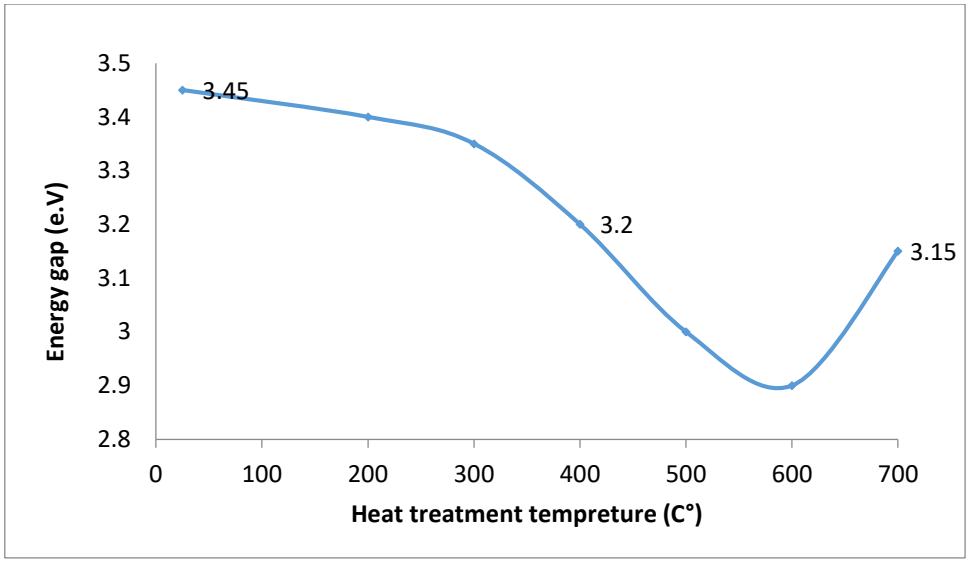

Figure 5. Energy gap as a function of treatment temperatures.

3. 3 Structural Properties

The purpose of annealing is to produce a refined grain, to induce softness, improve electrical and magnetic properties, and sometimes to improve machinability.

X-ray diffraction profile of Nb_2O_5 thin films before and after heat treatments are shown in Figure 6 for different selected annealing temperatures.

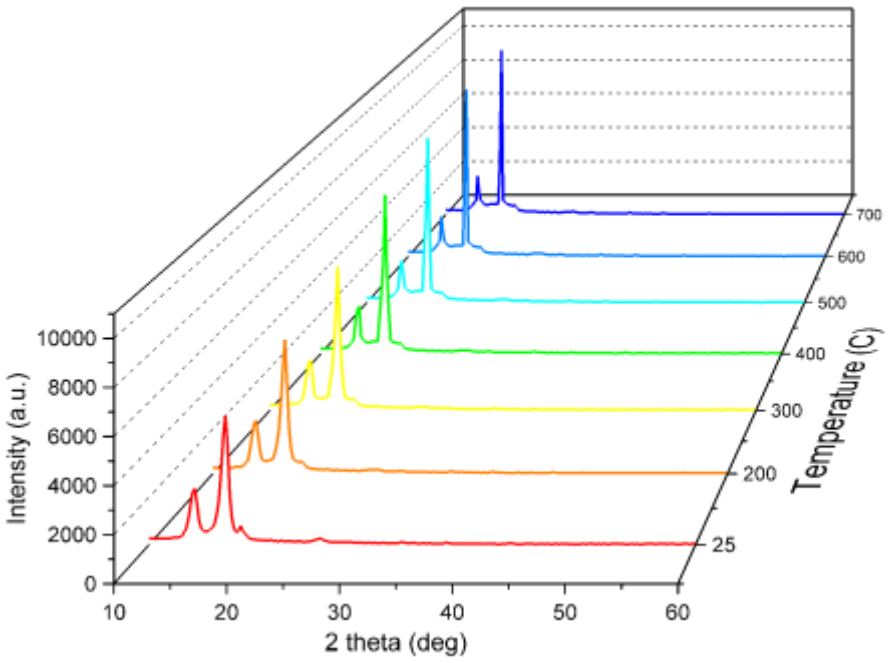

Figure 6. XRD results of the Nb_2O_5 film at different treatment temperatures.

The enhancement in the crystal growth and crystallization with treatment could be clearly recognized. In addition, no remarkable change in the diffraction peak position and no new material peak have appeared within the heat treatment. The obtained patterns were compared with (00-037-1468) standard cards.

The diffraction peak at 2θ= 17.20 which diffracted from (301) diffraction plane was obviously enhanced with annealing temperatures since it seems to be sharper after treatment. In addition, the diffraction peak at 2θ= 14.20, which is related to the (-203) diffraction plane, has a relative intensity reduction, the low diffraction peak related to the (-403) plane at 2θ= 18.80 was disappeared completely at 300 °C. The above results agreed with published data in [51]. Crystallite size, dislocation densities, and stress were estimated using equations (3-5), the results have been tabulated in Table 2.

From the obtained results it's clear that the grain size was increased from (9.48 to 34.71) nm as the temperature increased from 200 to 600°C, this is related to the particle growth and agglutination with each other through in the process of the heat treatment. As the temperature increased, the particle energy increased and as a result, they agglomerated with each other to convene larger particles [52, 53]. In metal oxides, there are many dangling bonds related to the metal and oxygen defects located at the grain boundaries.

As a result, these defects are favourable to the merging process to form larger grains when increasing the annealing temperature [54]. The stress value decreased with the annealing temperature from (0.23) to (0.06) as a result of the increase in the heating temperature. In fact,a relaxation in the Nb_2O_5 film appeared to occur in this case and that may be related to the reduced imperfections during the deposition process since the material molecule was deposited with a few disordering [55]. The density of dislocation also decreased with temperature which indicates for a reduction in the lattice imperfections concentration [56].

A relative reduction has been seen in the crystallite size after increasing the annealing temperature to 700 ^{o}C. This results in breaking the chemical bond between Nb and oxygen instead of enabling the atoms to take their corresponding sites resulting in producing further defects and more stress, [57] this is inconsistent with published data [57, 58]. In general, the annealing treatment increases the system's strength by reducing dislocation emission sources and improves material ductility by strengthening grain boundaries' resistance to intergranular cracks. The full annealing process consists of heating to the proper temperature and then cooling slowly, through the transformation range, in the furnace.

Table 2 Estimated structural constants

Temperature C°	**Grain size nm**	**Crystal Stress ε**	**Dislocation -density 1/nm²**
Room temperature	9.48	0.23	1.12E^{-02}
200	9.95	0.22	1.02E^{-02}
300	10.91	0.20	8.42E^{-03}
400	12.77	0.17	6.13E^{-03}
500	17.09	0.13	3.44E^{-03}
600	34.71	0.06	8.31E^{-04}
700	33.91	0.07	8.71E^{-04}

4. CONCLUSION

Nb_2O_5 thin film as a transparent conducting oxide was prepared successfully via the precipitation method and deposited by spin coating. The optical transmittance reached about 95% after heat treatment. High stoichiometric Nb_2O_5 thin film (72.98%) was prepared and enhanced using post heat-treatment to be about (76.2%). The surface morphology revealed a uniform surface that was free of cracks and voids which can be incorporated into optoelectronic application in future work

ACKNOWLEDGMENTS

The authors would like to thank the Applied Science Department, University of Technology-Iraq for the logistic support this work.

REFERENCES

[1] Aegerter, M. A., S. Sol Energy Mater Sol Cells. vol 68 (2001) p 422.
[2] Salim, E.T., Saimon, J.A., Abood, M.K., Fakhri, M.A., Mater. Res. Express, vol 6 issue 4 (2019) pp. 046420.
[3] Lazarova, K., Vasileva, M., Marinov, G., Babeva, T., Optics & Laser Tech., vol 58 (2014) pp. 114-118.
[4] Carniti P, Gervasini A, Marzo M. Dispersed NbOx catalytic phases in silica matrixes: influence of niobium concentration and preparative route. J Phys Chem C, vol 112 (2008) p. 14064.
[5] Ramírez, G., Rodil, S.E., Muhl, S., Ortega, D.T., Olaya, J.J., Rivera, M., Camps, E., Alarkon, L.E., J. non-crystalline Solids, vol 356 (2010) pp. 2714-2721.
[6] Fakhri, M. A., Salim, E. T., Wahid, M.H.A., Abdulwahhab, A. W., Hashim, U., Salim, Z. T., Optik, vol 180 (2019) pp. 768-774.
[7] Viet, A.L., Reddy, M., Jose, R., Chowdari, B., Ramakrishna, S., The J. Phys. Chem. C, vol 114 (2009) p. 664-671.
[8] Abood, M., Salim, E.T., Saimon, J.A., J. Ovonic Res., vol 15 issue 2 (2019) pp. 109 – 115.
[9] Ahn, K. S., Kang, M. S., Lee, J. K., Shin, B. C., Lee, J. W., Appl Phys Lett, vol 89 (2006) p. 013103.
[10] Abood, M.K., Wahid, M.H.A., Salim, E.T., Saimon, J.A., EPJ Web of Conf., vol 162 issue 12 (2017) p. 01058.
[11] Bhembe, Y., Lukhele, L., Ray, S., Dlamini, L., Dalton Transactions, vol 49 no 22, (2020) p. 7474.
[12] Ismail, R. A., Fakhri, M. A., Rasheed, B. G., Salim, Z. T., Iranian Journal of Science and Technology, Transactions A: Science, vol 43 issue 3 (2019) pp. 1337–1343
[13] Coşkun, Ö.D., Demirela, S., Appl. Surf. Sci., vol 277 (2013) pp. 35-39.
[14] Al Wazny, M. S., Salim, E. T., Bader, B. A. Fakhry, M. A. IOP Conference Series Materials Science and Engineering, vol 454 issue 1 (2018) p. 012160.
[15] Viet, A.L., Jose, R., Reddy, M., Chowdari, B., Ramakrishna, S., The J. Phys. Chemistry C, vol 114 (2010) pp. 21795-21800.
[16] Salim, E.T., Saimon, J.A., Abood, M.K., Fakhri, M. A, Optical and Quantum Electronics, vol 52 issue 10 (2020) p. 463
[17] Michalkiewicz, B., Nazzal, J.S., Tabero, P., Grzmil, B., Narkiewicz, U., Chemical Papers, vol 62 (2008) pp. 106-113.
[18] Taleb, S.M., Fakhri, M.A., Adnan, S.A., J. Ovonic Res., vol 15 issue 4 (2019) pp. 261 – 269.
[19] Michel, A., Sol. Energy Mater. Sol. Cells, vol 68 (2001) pp. 401-422.
[20] Hota, M., Bera, M., Verma, S., Maiti, C., Thin Solid Films, vol 520 (2012) pp. 6648-6652.
[21] Badr, B. A., Numan, N. H., Khalid, F. G., Fakhri, M. A., Abdulwahhab, A. W., Journal of Ovonic Research, vol 15 issue 1 (2019) pp. 53-59

[22] Masse, J.P., Szymanowski, H., Zabeida, O., Amassian, A., Sapieha, J.K., Martinu, L., Thin Solid Films, vol 515 (2006) pp. 1674-1682.
[23] Tamang, R., Varghese, B., Mhaisalkar, S.G., Tok, E.S., Sow, C.H., Nanotechnology, vol 22 (2011) p. 115202.
[24] Raba, A., Ortega, J.B., Joya, M., Applied Physics A, vol 119 (2015) pp. 923-928.
[25] Abood, M.K., Salim, E.T., Saimon, J.A., International Journal of Nanoelectronics and Materials, vol 11 (Special Issue BOND21) (2018) pp. 55-64
[26] Zhao, Y., Zhou, X., Ye, L., Tsang, S.C.E., Nano Reviews, vol 3 (2012) p. 17631.
[27] Ayanda, O.S., Adekola, F.A., J. Minerals and Mater. Characterization and Eng., vol 10 (2011) p. 245.
[28] Wang, X.H., Zheng, S.L., Xu, H.B., Zhang, Y., Transactions of Nonferrous Metals Society of China, vol 20 (2010) pp. 2006-2011.
[29] Aspart, A., Antoine, C., Appl. Surf. Sci., vol 227 (2004) pp. 17-29.
[30] Fakhri, M.A., Salim, E.T., Hashim, U., Abdulwahhab, A.W., Salim, Z.T., J. Mater. Sci.: Mater. in Electronics, vol 28 issue 22 (2017) pp. 16728-16735.
[31] Fakhri, M.A., Abdulwahhab, A.W., Kadhim, S.M., Alwazni, M.S., Adnan, S.A., Mater. Res. Express, vol 6 issue 2 (2018) p. 026429.
[32] Badr, B.A., Mohammed, Q.Q., Numan, N.H., Fakhri, M.A., AbdulWahhab, A.W., International J. Nanoelectronics and Mater., vol 12 issue 3 (2019) pp. 283-290.
[34] Abdul-Hamead, A. A., Othman, F. M., Fakhri, M. A., Journal of Materials Science: Materials in Electronics, vol 32, (2021) pp.15523–15532.
[35] Ismail, R. A., Rasheed, B. G., Salim, E.T. Al-Hadethy, M., Journal of Materials Science: Materials in Electronics, vol 18 issue 4 (2007) pp. 397-400.
[36] Hattab, F., Fakhry, M., 2012First National Conf. for Eng. Sci. (FNCES), (2012) pp. 1-5.
[37] Fakhri, M.A., International Journal of Nanoelectronics and Materials, vol 9 issue 1 (2016) pp 93-102.
[38] Bader, B.A., Numan, N.H., Khalid, F.G., Fakhri, M.A., Abdulwahhab, A.W., J. Ovonic Res., vol 15 issue 2 (2019) pp. 127-133.
[39] Salim, E.T., Surface Review and Letters, vol 20 issue 05 (2013) pp. 1350046.
[40] Muhsien, M.A., Salem, E.T., Agool I.R., Hamdan, H.H., Appl. Nanoscience, vol 4 (2014) pp. 719–732.
[41] Agool, I.R., Salim, E.T., Hassan, M.A., Int. J. Modern Phys. B, vol 25 issue 8 (2011) pp. 1081–1089.
[42] Ibraheam, A.S., Rzaij, J.M., Fakhri, M.A., Abdulwahhab, A.W., Mater. Res. Express, vol 6 issue 5 (2019) pp. 055916.
[43] Fakhri, M. A., Salim, E. T., Wahid, M.H.A., Abdulwahhab, A. W., Hashim, Z. T., U., Salim, Journal of Physics and Chemistry of Solids, vol 131 (2019) 180-188.
[44] Hassana, M.A.M., Al-Kadhemyb, M.F.H., Salem, E.T., Int. J. Nanoelectronics and Mater., vol 8 issue 2 (2015) pp. 69-82.
[45] Salem, E.T., Al-Wazny, M. S., Fakhri, M. A., Modern Physics Letters B, vol 27 issue 16 (2013) 1350122.
[46] ElZawawi, I., Mahdy, M.A., El-Sayad, E.A., J. Nanomaterials, vol 2017 (2017) pp. 1-14.
[47] Hafiz, M., El-Kabany, N., Kotb, H.M., Bakier, Y., Int. J. Thin. Fil. Sci. Tec., vol 4 (2015) pp. 163-171.
[48] Rao, T.P., Kumar, M.S., Ganesan, V., Indian J. Physics, vol 85 (2011) p. 1381.
[49] Mallika, A., Reddy, A.R., Reddy, K.V., J. Advanced Ceramics, vol 4 (2015) pp. 123-129.
[50] Pandey, S.K., Pandey, D.S.K., Awasthi, V., Kumar, A., Deshpande, U.P., Gupta, M., Mukherjee, S., Bulletin of Mater. Sci., vol 37 (2014) pp. 983-989.
[51] Ivanova, T., Harizanova, A., Koutzarova, T., Vertruyen, B., Mater. letters, vol 64 (2010) pp. 1147-1149.
[52] Coşkun, Ö.D., Demirel, S., Atak, G., J. Alloys and Compounds, vol 648 (2015) pp. 994-1004.
[53] Goldenberg, E.Ç., Sapieha, J.E.K., Martinu, L., Appl. Optics, vol 51 (2012) pp. 6498-6507.
[54] Ismail, R.A., Hamoudi, W.K., Abbas, H.F., Mater. Res. Express, vol 5 (2018) p. 025017.

[55] Somnath, M., Asit, K. K., Journal of Science: Advanced Materials and Devices, vol 2 issue 2 (2017) pp. 165-171
[56] Ismail, R. A., Salim, E. T., Hamoudi, W. K., Materials Science and Engineering C, vol 33 issue 1 (2013) pp. 47-52.
[57] Chen, L., Deng, H., Tao, J., Zhou, W., Sun, L., Yue, F., Yang, P., Chu, J., Journal of Alloys and Compounds, vol. 640, (2015) pp. 23-28.
[58] Barranco, A., Borras, A., Gonzalez-Elipe, A. R., Palmero, A., Progress in Materials Science, vol. 76 (2016), pp. 59-153